Corrosion Characteristics of Studsvik R2 Al-Alloy by Hydrogen Evolution Under Simulated Repository Conditions – 25123

Marvin Schobel *, Christian Ekberg *, Teodora Retegan Vollmer *, Anders Puranen **

* Chalmers University of Technology

** AB Svafo / Chalmers University

ABSTRACT

Large quantities of low and intermediate level radioactive waste are produced by the dismantling of nuclear reactors. It must be kept confined to ensure safety for extended time scales. To ensure this, the waste can be encapsulated in concrete which makes the interim storage and repository conditions alkaline (pH > 12). This is advantageous for some heavy-element radionuclides because it fosters their precipitation. For reactive metals and their corrosion characteristics, however, it can be problematic. The Swedish Studsvik R2 nuclear research reactor build contained an AlMg3.5 alloy similar to Al 5154 for its core internals and the reactor tank. The corrosion of aluminum at alkaline conditions is known to start at exorbitant high levels and then decrease very rapidly due to the formation of a protective oxide layer on the surface of the sample. The formation of corrosion products leads to a potential volume expansion which is accompanied by the evolution of hydrogen gas and the following pressure build-up. Both can lead to cracks in the concrete which creates possible pathways for radionuclides. Unirradiated rod-shaped samples were cut from a reference sample originating from the manufacture of the reactor vessel. Samples were embedded in regular Portland cement concrete with an elevated water/cement ratio of 0.7 to ensure the availability of water throughout the experiment due to increased pore water content. The embedded samples were put into overpressure bottles alongside pressure, humidity & temperature sensors. Corrosion rates were calculated from the evolving hydrogen pressure inside the bottle. Samples of the same geometry, from pure aluminum (99.95 %) were also used as references. The R2 alloy had an initial corrosion rate of 564 (± 180) µm during the first two weeks and then decreased to 434 (± 178) µm/y after one month. The reference material had a corrosion rate of 1622 (± 283) µm/y during the first two weeks and decreased to 606 (± 222) µm/y after one month which suggests a trend of the R2 alloy corroding slower than pure aluminum.

INTRODUCTION

Low- and intermediate-level radioactive waste is generated during the decommissioning of nuclear reactors [1]. Materials of this type must be disposed properly to ensure safety for the environment and public, which requires extended lifetimes of these repositories [2]. Therefore, high requirements for resistance to both natural degradation processes and waste-induced alteration processes are required [2]. The decommissioning waste as well as other low- and intermediate-level waste products can be processed by encapsulation in concrete as a barrier, providing high pH and low permeability [3]. These alkaline conditions are known to be beneficial for the long-term retention of radionuclides due to sorption and limited solubility [3-5]. However, the high pH value of 12.5 or higher associated with concrete porewater, which decreases over time to below 10, can have a detrimental effect on the corrosion properties of reactive metals such as aluminum [1, 4, 6].

Aluminum along with its alloys is sometimes used particularly in nuclear research reactors [1]. It is known to exhibit rapid initial corrosion rates under alkaline conditions due to the early formation of a passivation layer by oxidation on the surface. This oxide layer prevents the material from corroding as quickly and thus slows the further formation of aluminum oxides and hydroxides in a magnitude of seconds to weeks, depending on the surface of the material [1, 6]. Solid corrosion products under repository conditions are mostly amorphous Al₂O₃ in the early stage and Al(OH)₃ after formation of the

oxide layer according to equations (1) and (3) at pH values higher than 12 [1, 6-8]. The formation of the Al(OH)₄- ion, which is the dominating phase, as given in equation (4) is assumed to be the main reason for a later dissolution of the oxide layer at high pH [8]. Volume expansion due to the formation of oxidation products and hydrogen gas [1, 4, 6, 9, 10] build up pressure that can lead to cracks in the concrete, which thus act as pathways for radionuclides that may challenge the long term safety assement of the repository[1, 2].

$$2Al + 3H_2O \rightarrow Al_2O_3 + 3H_2$$
 (Eq. 1)

$$2Al + 4H_2O \rightarrow 2AlOOH + 3H_2$$
 (Eq. 2)

$$2Al + 6H_2O \rightarrow 2Al(OH)_3 + 3H_2$$
 (Eq. 3)

Only a few studies have been conducted in which aluminum corrosion was investigated under repository or repository-like conditions. However, these studies confirmed high initial corrosion rates in the order of 10³ µm/y after two weeks to 20 days [1, 6]. These rates quickly slowed down, attributed to protection of the metal by the passivation layer and reached values in the order of 10² µm/y after time spans of only 26 to 80 days. Previous studies mostly used electrochemical methods [e.g., 7, 10] or mass loss evaluation [e.g., 1, 6, 11] to investigate the corrosion rates of aluminum under alkaline conditions. It is known that the corrosion of aluminum is not affected by the presence of oxygen [12].

The reactor build of the decommissioned Studsvik R2 contained an AlMg3.5 alloy for its core internals and reactor tank with a similar composition as Al5154. As the magnesium content is less than 7 %, stress corrosion cracking of the material can be excluded from any considerations [13]. However, the additional evolution of hydrogen gas should be considered as it is a known by-product of magnesium corrosion [e.g.,14, 15-18]. Since there is no data on this particular alloy, its corrosion properties were investigated in this study. For this purpose, rods cut from the original AlMg3.5 alloy batch of the decommissioned R2 reactor were corroded simulating generic conditions of a Swedish repository for low- and intermediatelevel radioactive waste by conducting the experiment in a glovebox under unaerated conditions at room temperature (approximately 21 °C).

MATERIALS AND METHODS

Sample preparation

Rod-shaped samples measuring 15 mm in length and 5 mm in diameter were cut and machined from unirradiated reference samples from the fabrication of the Studsvik R2 reactor tank. Samples with the same dimensions were produced from pure aluminum (99.95 %, Thermo Scientific Chemicals, USA). The geometric surface was used in the calculations, as the small surfaces of the rods proved difficult to measure by the BET instrument available in our lab. The average roughness factors caused by machining should not change the order of magnitude of the results, especially given that the evolution of surfaces by the corrosion process would probably induce a larger change in surface area.

Concrete and cement water

250 g of concrete was produced by mixing 65.8 g of standard CEM 1 Portland cement (Chalmers Building Materials Lab, Sweden), 13.2 g of calcium carbonate (Limus 40, Nordkalk, Sweden), 132 g of standard sand (EN 196-1 standard sand) and 46.1 ml of MO water. With a water-cement ratio of 0.7, a slightly higher value was aimed for than for conventional concrete, as the availability of water should be ensured in order to guarantee the continuation of corrosion due to increased pore water content. The cement water (CW) was prepared by dissolving 0.74 g NaCl in 200 ml MO water. Perforated 3-ml Eppendorf tubes contained about 0.43 g CaO to ensure a constant pH of above 12. The pH value was confirmed with a pH paper. The Eppendorf tubes were immersed in the CW solution.

Sensor modification

Temperature, humidity and pressure sensors (T1, Aqara, China) were dismantled. As the usual button cell for this type of sensor only lasted a few weeks under the humid and salty experimental conditions, a double AA battery pack was soldered to each sensor as a replacement. The sensor boards were coated to prevent failure due to moisture induced corrosion (Figure 1).



Figure 1: Modified pressure sensor with attached battery pack.

A Raspberry Pi single board computer (Zero WH v.1.1, Raspberry Pi Ltd., UK) was set up with a Zigbee-based broker and a Zigbee coordinator (CC2652R, Slaesh GmbH, Germany) was connected via USB. A Python script was written and used to automatically collect data from the modified sensors. The sensor wirelessly sent data when changes were detected.

Experimental setup

All experiments were carried out in triplicates in an inert glovebox (typically <0.1 ppm O_2) filled with nitrogen to prevent aeration or hydrogen combustion and to create stable repository-like conditions (approximately 21 $^{\circ}$ C).

In concrete: 5 ml of concrete was filled into a 30 ml vial. The samples were immersed in the middle of the concrete layer which hardened for about five minutes until stable. The vial was filled up to 20 ml with concrete. It was then carefully filled into a 500 ml GL45 overpressure bottle (pressure plus+, DURAN Group GmbH, Germany) along with a modified sensor (T1, Aqara, China). The overpressure bottles can withstand an overpressure of up to 1.5 bar, and the sample size was selected so that the pressure build-up does not reach the limit even if the material would corrode completely. A silicone septum was used for the first tests. As it began to leak after a few weeks, it was replaced by a bromobutyl septum (DURAN group GmbH, Germany) in order to seal the bottle tightly and to be able to take gaseous (or liquid) samples when continuing the experiments. The bottle was sealed with a lid (DURAN group GmbH, Germany) (Figure 2a). The experiment was conducted in triplicate and repeated with pure aluminum as a reference.

In CW: A 30 ml vial was filled with 20 ml of the prepared CW with the CaO-containing Erlenmeyer tube. The samples were immersed in the CW and then added to the vial along with a modified sensor. The bottle was sealed with a bromobutyl septum and closed with a lid (Figure 2b). The experiment was performed in triplicate and repeated with pure aluminum as a reference. Data was collected over a period of up to 8 months.

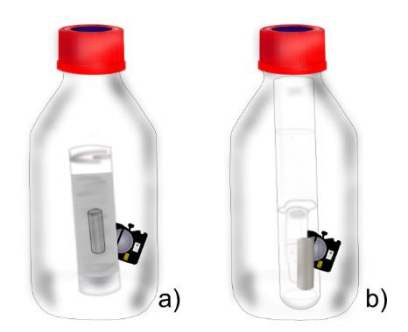


Figure 2: Experimental setup. a) Vial with sample immersed in concrete in overpressure bottle with bromobutyl septum and lid. b) Vial with sample immersed in CW with pressure sensor in bottle with bromobutyl septum and lid.

Calculation of corrosion rates

Equations (1) - (4) were assumed for the calculation of the corrosion rates with aluminum oxide as an early formed passive protective layer (Al_2O_3) and aluminum hydroxide $(Al(OH)_3)$ as solid corrosion products. Since no detailed surface analysis has been performed, only solid corrosion products of the same density as aluminium were assumed for the calculation of the surface layer thickness.

The sensors recorded each pressure increase. The pressure changes were then used to calculate the amount of substance n H₂ and furthermore n Al. The mass m Al could then be calculated using the molar mass M of Al. Based on m Al, the corrosion rate was calculated in units of $g/m^2/y$. By including the surface area of the samples, it was also possible to calculate the corrosion depth and thus the corrosion rates in μ m/y. The corrosion rates were calculated as average values for specific time periods between days and weeks, depending on the duration of the experiment. Uncertainties are given by the differences between replicates and deviations in between the averaging time periods. Corrosion rates presented in this paper are calculated as averages from a variable timestep ranging from days at the start of the experiments to weeks at longer exposures. The rates are thus not cumulative from the start of the experiment.

Analytical Methods

The relative element concentrations in the alloy and oxide were measured with a portable XRF device (Niton XL5 Plus Thermo Scientific, USA). As this was an exploratory test, no replicates were measured. The measurements were carried out for samples corroding in the CW solution by temporarily lifting the samples out of the solution, rinsing with MQ water, measuring and returning the samples to the CW solutions.

RESULTS

Corrosion rates



Figure 3: Rapid hydrogen evolution on the surface of the R2 alloy in CW.

Figure 3 shows a sample rod of the R2 reactor alloy immediately after starting the experiment caused by the rapid hydrogen evolution while forming the oxide layer. Figure 4 shows the calculated corrosion rates in μ m/y of the R2 reactor vessel alloy and a pure aluminum metal as a reference for a period of four weeks in concrete including an insert over lower corrosion rates and a shorter time span. While some of the sensors stopped working, those samples could still be used for mass loss evaluation and analysis of the corrosion products. Standard deviations in all figures were calculated from triplicates and averages over the specific time intervals. The data was extrapolated to 24 weeks with a power fit, considering data from individual samples run over longer periods of time. The initial corrosion rates for both the R2 alloy and the metal are immediately in the order of hundreds of thousands μ m/y (outside the scale of Figure 4) and have high uncertainties caused by the immediate onset of corrosion, which varies due to slight variations in sample preparation and the calculation of time-dependent averages of corrosion rates. Rates for both materials start to drop sharply after the first few hours, then level off and drop to a corrosion rate of 434 (±178) μ m/y after 4 weeks for the R2 alloy. The rate of pure aluminum slowed down to 606 (±222) μ m/y after 4 weeks. The fit also confirms the trend that the aluminum metal corrodes faster than the R2 alloy.

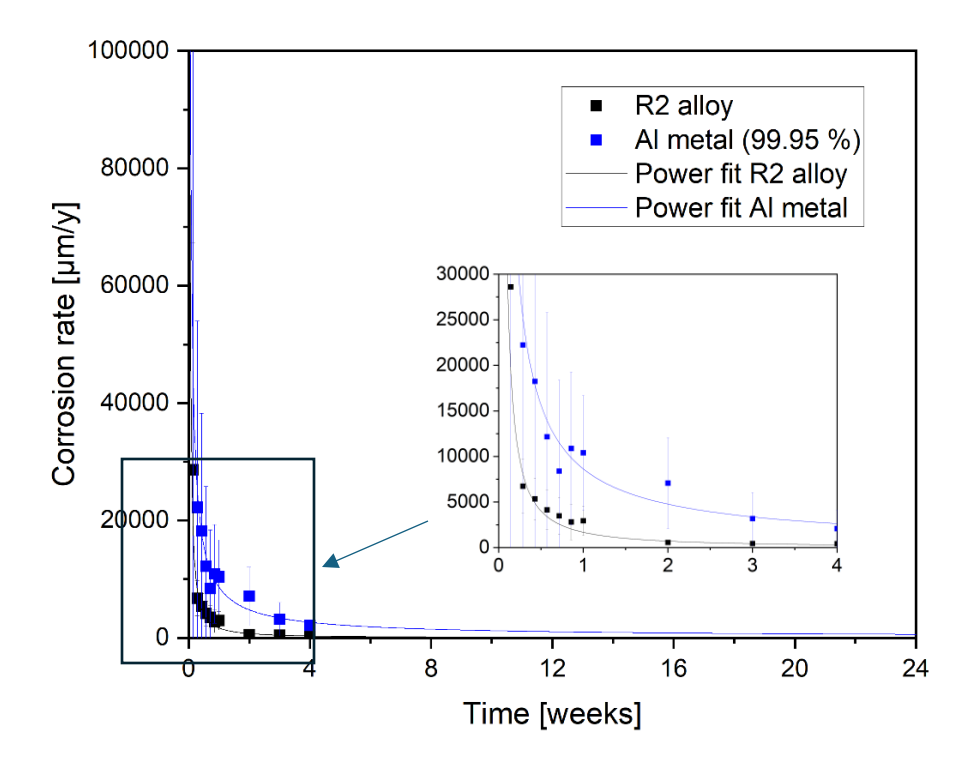


Figure 4: Corrosion rates and extrapolation of R2 reactor alloy and aluminum metal up to 24 weeks in concrete. Insert on lower corrosion rates.

Figure 5 shows the corrosion rates of the R2 reactor alloy and the pure aluminum metal in artificial cement water over a period of 24 weeks. The initial corrosion rates are extremely high and subject to large uncertainties, which was also observed for the samples in concrete. The missing data between weeks 4 and 16 is due to a change in the sensor's battery system. The corrosion rate of the R2 reactor alloy decreased to 397 (\pm 114) μ m/year, while that of the pure aluminum decreased to 458 (\pm 127) μ m/year after 24 weeks. The power fit also slightly indicates a trend for the aluminum metal to corrode faster than the R2 alloy as the curve flattens out with longer term corrosion.

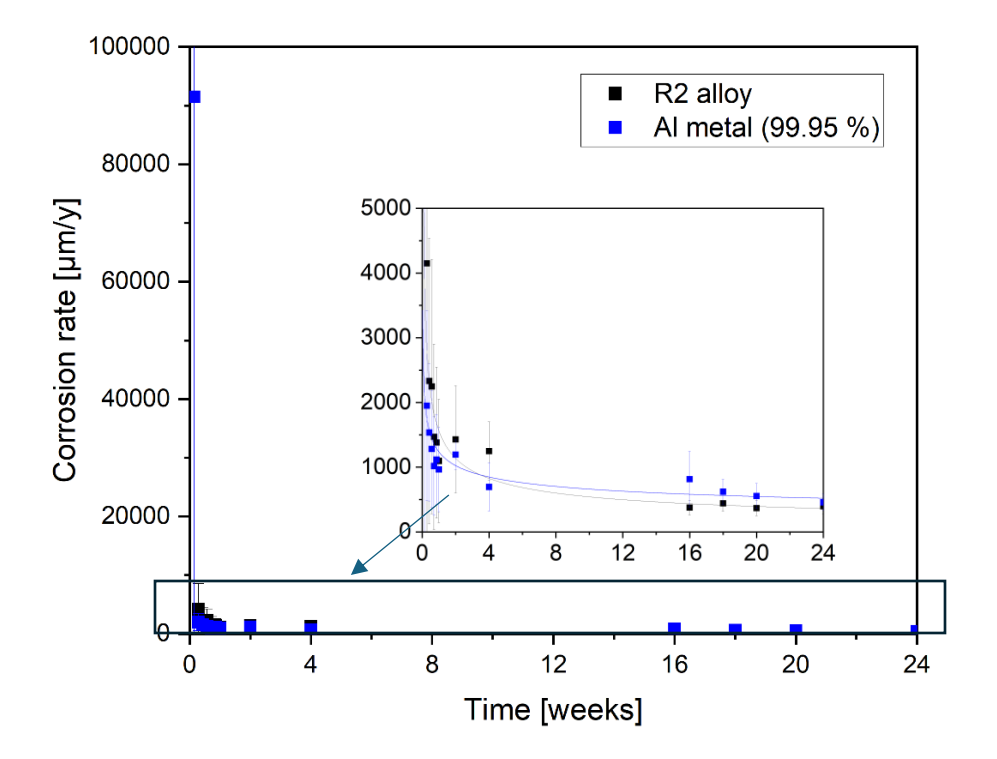


Figure 5: Corrosion rates of R2 reactor alloy and aluminum metal up to 24 weeks in CW. Insert on lower corrosion rates.

Oxide layer thickness

The thicknesses of the surface layers of the samples were calculated from the hydrogen evolution and can be seen in Figure 6. The R2 reactor alloy in concrete had a layer thickness of $20~(\pm 2)~\mu m$ after 2 weeks and a thickness of $33~(\pm 6)~\mu m$ after 4 weeks. For CW, the actual rates after 24 weeks can only be estimated as the sensors did not measure when the battery method was changed. Open symbols are single samples without replicates. The R2 alloy had a calculated layer thickness of $62~(\pm 6)~\mu m$ after 2 weeks and more than $78~(\pm 26)~\mu m$ after 24 weeks. Pure aluminum had a surface layer thickness of $41~(\pm 8)~\mu m$ after 2 weeks and $46~(\pm 3)~\mu m$ after 4 weeks in concrete and $49~(\pm 5)~\mu m$ after two weeks and $136~(\pm 40)~\mu m$.

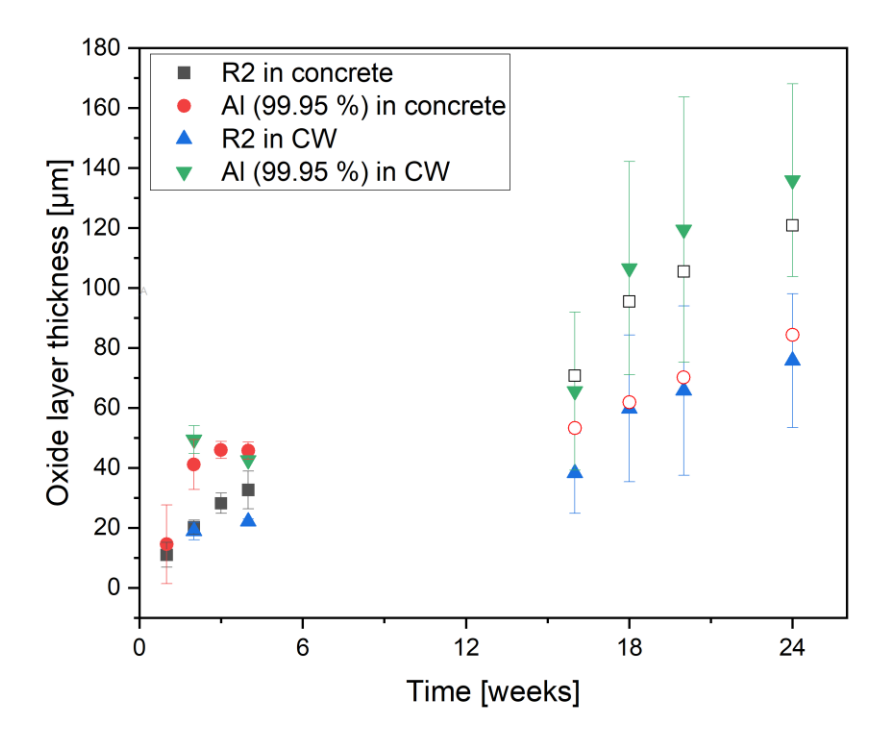


Figure 6: Calculated layer thickness of the R2 alloy and pure aluminum in concrete and in CW.

Element analysis

Table 1 shows the relative element concentrations of aluminum, chromium, magnesium, iron and silicon in the original alloy and after four and eight months of corrosion in CW. The concentrations were measured with a portable XRF device. Unusually high element concentrations were measured for some elements as the samples were measured in situ without disrupting the exposure time. The measured aluminum concentration is higher after 8 months than after 4 months. The chromium concentration decreases from 4 to 8 months. The magnesium concentration decreases until it is no longer detectable after 8 months. The iron concentration also decreases after 8 months, and the silicon concentration remains almost unchanged.

Table 1: Relative element concentration of Al, Cr, Mg, Fe, and Si of original sample and after 4 and 8 months (LOD = Limit Of Detection).

	Initial composition	4 months exposure	8 months exposure
Element	%	%	%
Al	95.7 ± 0.13	92.3 ± 0.44	96.3 ± 0.20
Cr	0.23 ± 0.00	2.04 ± 0.05	0.68 ± 0.01
Mg	3.52 ± 0.13	1.57 ± 0.51	LOD < 0.3
Fe	0.29 ± 0.01	1.55 ± 0.07	0.99 ± 0.03
Si	0.13 ± 0.02	1.25 ± 0.15	1.48 ± 0.08

DISCUSSION

Corrosion rates

In the beginning of the experiments, high corrosion rates with very high uncertainty were observed. This can be attributed to various factors in the test setup and in the data analysis. The sample begins to corrode immediately when it comes into contact with the concrete. As the experiments were conducted in an inert glovebox, the preparation time and therefore the differences in preparation time may be longer than when conducted on the benchtop, leading to differences in the measured hydrogen pressure of the triplicates and therefore differences in the calculated corrosion rates. Since the experiments were planned to provide information on long-term rates, the corrosion rates were calculated as time-dependent averages, which also leads to uncertainties. However, in the long term, which is the focus of this work, the uncertainties level out at low values. The trend of immensely high corrosion rates at the beginning of the experiment is clearly visible and can be explained by the fact that an aluminum oxide layer on the surface has not yet formed on the samples [1, 6, 7]. By immediately measuring the pressure, the actual extent of the initial corrosion rates becomes clear.

Corrosion rates begin to decrease quickly for both pure aluminum and the R2 alloy in CW and concrete. The rapid decrease is consistent with the newly formed oxidation layer protecting the samples and resulting in less available surface area [1, 6]. The wetted surface area could also be affected by the degree of attached gas bubbles potentially impacting the initial corrosion rates. After a few weeks, corrosion rates continue to decrease, but at a very slow rate consistent with the power law, as previously suggested in the literature [19].

The corrosion rates of the samples in concrete (Figure 4) slowed down less rapidly than in the CW (Figure 5), which could indicate less aggressive conditions in the concrete. In addition, the long-term trend of corrosion rates in concrete (Figure 4) indicates faster corrosion trends for the aluminum metal compared to the R2 reactor alloy, most likely due to the purity of the rapidly corroding aluminum under alkaline conditions [1, 4, 6, 9, 10]. In CW, pure aluminum and the R2 reactor alloy show similar corrosion rates. However, there is a slight trend that is consistent with the results of the experiment in concrete. The calculated surface layer thicknesses also indicate faster corrosion of pure aluminum in both concrete and CW.

Layer thickness

The oxide layer thicknesses are consistent with the trend of pure aluminum corroding faster than the R2 reactor alloy in CW. No conclusions can be drawn about the corrosion in concrete and the similarity of the conditions in CW and concrete as the samples in concrete are not available in replicates for data over longer periods of time and the values are within a possible uncertainty range.

Element analysis

The results of the XRF measurement indicates that with increasing exposure time, a decrease in the relative magnesium concentration and an increase in the aluminum concentration relative to the other analyzed elements, tabulated in Table 1. Considering the increasing thickness of the oxidation layer, this indicates that magnesium is not incorporated into the oxide layer. After 8 months, the oxidation layer is so thick that the XRF no longer measures any of the original alloy, i.e. no magnesium. Given the very low Mg X-ray energy (K α 1.25 keV) this effect is in line with the expected 99% Mg attenuation occurring for about 30 μ m of aluminum thickness given the unknown attenuation through the oxide. The Mg(OH)₂ formed during the corrosion of the alloy may not be incorporated into the aluminum oxide layer because it is soluble [12, 14-18]. The oxide layer, however, appears to incorporate Cr, Fe and Si. This should be investigated further in future studies. It should also be mentioned that light elements such as oxygen and hydrogen cannot be detected by XRF.

CONCLUSION AND FUTURE RESEARCH

This study showed very high initial corrosion rates in both R2 alloy and pure aluminum, which for the latter is consistent with the literature. The extent of corrosion was clearly visible due to the immediate start of gas generation. The decrease of the corrosion rates for all samples was also consistent with the literature due to the formation of a protective layer. The results indicate a faster initial corrosion rate for pure aluminum, which is also supported by the calculated surface layer thicknesses of the triplicate samples in CW. To prove this, more long-term corrosion data is needed.

A decreasing magnesium content in the samples exposed to CW with increasing exposure time suggests that magnesium is not incorporated in the surface layer and can no longer be detected when the layer becomes too thick for the XRF to measure through. This must be proven by replicates, additional techniques such as electron microscopy and solution analysis.

In general, the investigation of the corrosion properties by measuring the hydrogen pressure in situ while the material continues to corrode is promising and should be further developed with a more stable sensor system. A new set of stainless vessels and pressure gauges adapted for hydrogen use is being commissioned. Final evaluation of the data will be done after more experiments with high resolution have been performed. Future experiments may include different materials and types of concrete for future repository solutions.

REFERENCES

- [1] G. Herting, and I. Odnevall, "Corrosion of Aluminium and Zinc in Concrete at Simulated Conditions of the Repository of Low Active Waste in Sweden," Corrosion and Materials Degradation, vol. 2, no. 2, pp. 150-163, 2021.
- [2] L. P. Santana, "Management of radioactive waste: A review," Proceedings of the International Academy of Ecology and Environmental Sciences, vol. 6, no. 2, pp. 38, 2016.
- [3] Strålsäkerhetsmyndigheten, "Kingdom of Sweden ARTEMIS. Self-assessment Report 2023", The IAEA Integrated Review Service for Radioactive Waste and Spent Fuel Management, Decommissioning and Remediation.

 (ARTEMIS)", Report number: 2023:04, 2023.
- [4] H. Kinoshita, P. Swift, C. Utton, B. Carro-Mateo, G. Marchand, N. Collier, and N. Milestone, "Corrosion of aluminium metal in OPC- and CAC-based cement matrices," Cement and Concrete Research, vol. 50, pp. 11-18, 2013.
- [5] M. Atkins, and F. Glasser, "Application of Portland cement-based materials to radioactive waste immobilization," Waste Management, vol. 12, no. 2-3, pp. 105-131, 1992.
- [6] M. Tabrizi, S. Lyon, G. Thompson, and J. Ferguson, "The long-term corrosion of aluminium in alkaline media," Corrosion science, vol. 32, no. 7, pp. 733-742, 1991.
- [7] H. Ezuber, A. El-Houd, and F. El-Shawesh, "A study on the corrosion behavior of aluminum alloys in seawater," Materials & Design, vol. 29, no. 4, pp. 801-805, 2008.
- [8] F. Xiao, R. Yang, and Z. Liu, "Active aluminum composites and their hydrogen generation via hydrolysis reaction: A review," International Journal of Hydrogen Energy, vol. 47, no. 1, pp. 365-386, 2022.
- [9] D. Jana, and D. G. Tepke, "Corrosion of aluminum metal in concrete—a case study." pp. 33-65.
- [10] S.-I. Pyun, and S.-M. Moon, "Corrosion mechanism of pure aluminium in aqueous alkaline solution," Journal of Solid State Electrochemistry, vol. 4, pp. 267-272, 2000.
- [11] M. Husaini, B. Usman, and M. B. Ibrahim, "Evaluation of corrosion behaviour of aluminum in different environment," Bayero Journal of Pure and Applied Sciences, vol. 11, no. 1, pp. 88-92, 2018
- [12] P. Mauret, and P. Lacaze, "Water corrosion studies of AlMg (5154) and AlCuMg (2024) aluminium alloys by gas chromatography," Corrosion Science, vol. 22, no. 4, pp. 321-329, 1982.
- [13] R. H. Jones, J. S. Vetrano, and C. F. Windisch, "Stress Corrosion Cracking of Al-Mg and Mg-Al Alloys, December 2004," Corrosion, vol. 60, no. 12, 2004.
- [14] S. Thomas, N. V. Medhekar, G. S. Frankel, and N. Birbilis, "Corrosion mechanism and hydrogen evolution on Mg," Current Opinion in Solid State and Materials Science, vol. 19, no. 2, pp. 85-94, 2015.
- [15] A. D. King, N. Birbilis, and J. R. Scully, "Accurate electrochemical measurement of magnesium corrosion rates; a combined impedance, mass-loss and hydrogen collection study," Electrochimica Acta, vol. 121, pp. 394-406, 2014.
- [16] M. Curioni, "The behaviour of magnesium during free corrosion and potentiodynamic polarization investigated by real-time hydrogen measurement and optical imaging," Electrochimica Acta, vol. 120, pp. 284-292, 2014.
- [17] Y. Yang, F. Scenini, and M. Curioni, "A study on magnesium corrosion by real-time imaging and electrochemical methods: relationship between local processes and hydrogen evolution," Electrochimica Acta, vol. 198, pp. 174-184, 2016.
- [18] G. Song, A. Atrens, and D. StJohn, "An hydrogen evolution method for the estimation of the corrosion rate of magnesium alloys," Essential readings in magnesium technology, pp. 565-572, 2016.
- [19] R. E. Melchers, Modelling the long term atmospheric corrosion of aluminium alloys, Research Report 278.04. 2010, The University of Newcastle, New South Wales ..., 2010.

WM2025 Conference, March 9 - 13, 2025, Phoenix, Arizona, USA

ACKNOWLEDGEMENTS

AB Svafo as well as the Swedish Nuclear and Fuel and Waste Management Co. are greatly acknowledged for funding of this research.